A NEW METHOD TO MEASURE MICRO CRACKS – THE UNDERESTIMATED INITIATORS OF DAMAGE TO COMPOSITE MATERIALS

K. Tazelaar [1*], S. Koussios[1], A. Beukers[1]

[1]*Faculty of aerospace engineering, department design and production of composite structures, technical university Delft, Kluyverweg 1, 2629 HS Delft, The Netherlands*
**k.tazelaar@tudelft.nl*

Keywords: carbon/epoxy composites, critical strain, curvature, test method

Abstract
Critical strain is a material constant and a critical parameter for many applications. It is not depending on temperature if no phase transition is involved. For composites only few publications on critical strain are known due to the fact that critical strain and crazes are not considered to cause fatal failure. New applications and combinations of composites with top layers have recently shown unforeseen damage modes which can be directly related to the critical strain of those materials. In this paper, the Euler-Fresnel spiral is introduced as a simple but reliable method to measure critical strains of composite materials at different temperatures and environments.

1 Introduction to the critical strain and it's determination for composite materials

Aeroplanes are covered by a nice furnish to protect the constructive materials. These protective layers have been improved during several decades to withstand environmental influences. Nowadays, aeroplanes are partly or fully made with composite materials, which are however showing odd reactions on the outer skin areas. Even though the composite materials have thoroughly been characterised in terms of mechanical properties and might not show fatigue in the traditional way of thinking, some little, not fatal damage, such as crazing followed by micro-cracking, may take place and trigger unforeseen degradation processes. Critical strain can be understood as a well-defined strain limit at which crazes and resulting irreversible micro cracks occur in the material without plastic deformation or breakage. It is not depending on temperature if no phase transition is involved [1].

1.1 Micro-cracks

Former research has proven that transverse cracks, even at levels of saturated crack density, reduce the stiffness, compressive and flexural strength of multidirectional laminates by less than 10% and therefore are not considered to be crucial in their effects on the structural performance [2, 3]. The process of micro-cracking is irreversible and initiated by crazing. The basic mechanism of craze initiation is starting with the formation of very small voids (< 30 [nm]). These voids can then grow and finally become crazes. Crazing has been studied fundamentally by many researchers [e.g. 4-6] and it is a well-known fact that crazes are no real cracks but thin spots in the material just about to crack due to disentanglement and

breakdown of the crazes. These micro cracks will, if not arrested, propagate to the surface and function as a notch for the top layers which will eventually show visible cracks. Therefore crazing and micro cracks must be considered as irreversible damage phenomena and a potential source of brittle fracture; thus they must be avoided in structural integrity critical applications [7].

1.2 Critical strain

Critical strain is often mentioned in the literature when problems occur in several applications which were not expected on the basis of the specifications concerning the involved material properties. For example, solvent stress cracking of plastics due to solvent exposure has been a topic to General Motors in the late 1970's [8]. Normally, critical strain is not an important design parameter because it does not give any information about fatal failure of a material. However, materials like carbon/epoxy composites in combination with top layers (and their broad variety of applications) force us to reconsider critical strain as a meaningful design / damage parameter.

2 Development of Euler-Fresnel spiral as valid test-method for critical strains

In the early 60's, Bergen has introduced a method to measure critical strains of polymers. The Bergen ellipse has mainly been used to measure critical strains for environmental effects, stress cracking and solvent crazing of plastics under certain applied stress levels [9, 10].
For composites the Bergen ellipse is not sufficient due to the fact that composites will show much lower critical strains than those of unfilled plastics. For the Bergen ellipse, the bending curvature (strain level) is not a linear function of the contour length hence its accuracy is limited; it is over-sensitive to high strains and prone to measurement mistakes in the range of low strains. On the other hand, the curvature of the Euler-Fresnel-curve, which is introduced here, is linear to the contour length and shows the same sensitivity to low and high strain levels. The following discussion is devoted to the development and comparison of the Bergen and Euler-Fresnel strain measurement methods:

2.1 Bergen-Elips versus Euler-Fresnel spiral

Let a curve **C** be given by:

$$\mathbf{C}(\theta) = \{x(\theta), \quad y(\theta)\}, \qquad \theta_0 \le \theta \le \theta_1 \tag{1}$$

The length along the curve, measured from point θ_0, is:

$$s(\theta) = \int_{\theta_0}^{\theta} \sqrt{\left(x'(t)\right)^2 + \left(y'(t)\right)^2}\, dt + \text{const} \tag{2}$$

The associated curvature is:

$$k(\theta) = \frac{1}{R(\theta)} = \frac{x'(\theta)y''(\theta) - y''(\theta)x'(\theta)}{\left(\left(x'(\theta)\right)^2 + \left(y'(\theta)\right)^2\right)^{3/2}} \tag{3}$$

An ellipse is for example described by:

$$\mathbf{C}_{\text{ell}}(\theta) = \{A\cos\theta, \quad B\sin\theta\} \tag{4}$$

Its curvature is:

$$k_{ell}(\theta) = \frac{AB}{(B^2\cos^2\theta + A^2\sin^2\theta)^{3/2}} \tag{5}$$

The Bergen ellipse [9] is based on A = 150 [mm] and B = 60 [mm], Fig. 1:

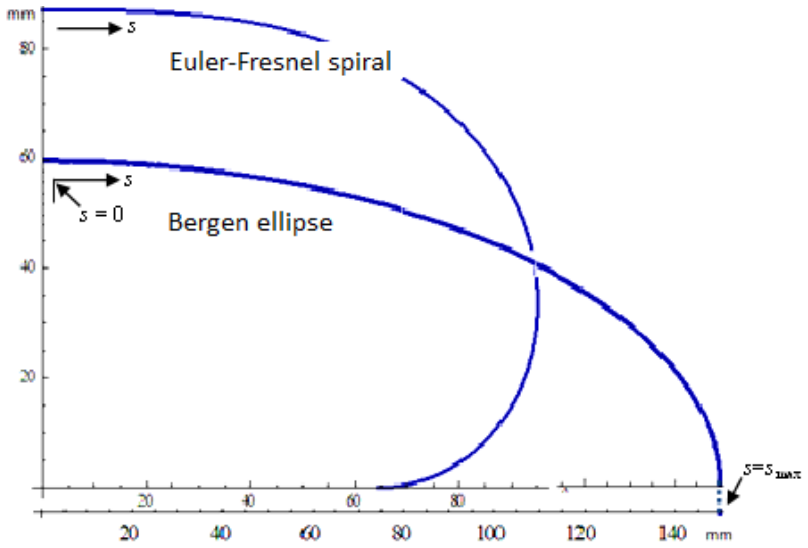

Figure 1. Euler-Fresnel curve for which the curvature is a linear function of the contour length [0, s_{max}] and curve representing the Bergen ellipse

The length of this specific curve, s_{max}, is equal to 172.598 [mm]. The associated curvature as a function of the contour length (starting at the top of the curve, see Fig. 1) is depicted below, Fig. 2.
The curvature distribution [k_{min}, k_{max}] over the length [0, s_{max}] is far from homogeneous. This strong non-linearity introduces significant measurement errors. Ideally, the curvature should be a linear function of the contour length:

$$k = 2as \tag{6}$$

where a has the dimension of [m^{-2}] and s is in [m]. With the aid of Eqs. (2) and (3) is can be deduced that:

$$\mathbf{C}(s) = \sqrt{\frac{2\pi}{a}}\left\{\mathrm{FS}\left(\frac{2a}{\pi}s\right),\quad \mathrm{FC}\left(\frac{2a}{\pi}s\right)\right\},\quad 0 \le s \le \sqrt{\frac{\pi}{a}} \tag{7}$$

where FS and FC are Fresnel integrals, respectively given by $\int \sin\left(as^2\right)ds$ and $\int \cos\left(as^2\right)ds$.
The corresponding spiral, presented in the same orientation as the ellipse (with the same length s_{max}) is also depicted in Fig. 1.
For the Euler-Fresnel curve, the total Bergen ellipse length, s_{max}, is reached by setting $a = \pi / s_{max}^2$. To compare the curvature developments over s, it is convenient that both shapes, the Bergen ellipse and the Euler-Fresnel curve, generate the same maximum curvature k_{max}; therefore we assume now that $a = k_{max} / 2s_{max}$. The associated curvature as a function of the

contour length (from $s = 0$ to $s = s_{max}$), together with the curvature of the Bergen ellipse, is depicted below:

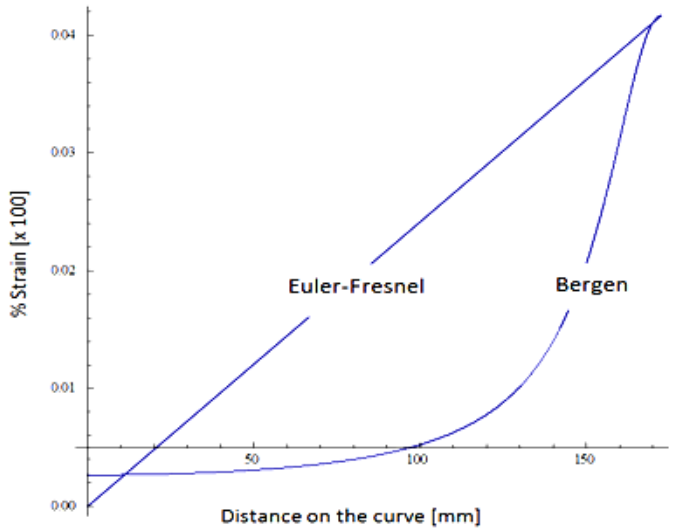

Figure. 2. Curvature as a function of curve length for the Bergen and the Euler-Fresnel curve

2.2 Strain formulation for the Euler-Fresnel curve

It is assumed now that a strip with width b and thickness t is placed over the Euler-Fresnel curve. The strain measurements take place on the outer surface of the strip (exposed side). Due to the thickness offset, the outer side of the strip will be forced to undergo a slightly modified curve:

$$\mathbf{C}(s) = \sqrt{\frac{2\pi}{a}}\left\{\mathrm{FS}\left(\frac{2a}{\pi}s\right),\quad \mathrm{FC}\left(\frac{2a}{\pi}s\right)\right\} + t\left\{-\cos(as^2),\quad \sin(as^2)\right\},\quad 0 \le s \le \sqrt{\frac{\pi}{a}} \tag{8}$$

The curvature of the outer side thus becomes:

$$k = \frac{2as}{1+2ast} \tag{9}$$

In general, the bending moment due to a curvature is:

$$M = kEI \tag{10}$$

where M is the bending moment, E the modulus of elasticity and I the second moment of inertia ($I = \frac{1}{12}bt^2$). The associated bending stress is:

$$\sigma = \frac{M\left(h - t/2\right)}{I}, \qquad 0 \le h \le t \tag{11}$$

With $\varepsilon = \sigma/E$ it can be derived that:

$$\varepsilon(h) = \frac{2as}{1+2ast}\left(h - \frac{t}{2}\right), \qquad 0 \le h \le t \tag{12}$$

The strain is thus linear to h and practically linear to s (since $t<<s$). The maximum tensile strain takes place on $s=\sqrt{\pi/a}$ (Eq. (8)) and $h=t$:

$$\varepsilon_{\max}=\frac{\sqrt{a\pi}}{\frac{1}{t}+2\sqrt{a\pi}} \tag{13}$$

To achieve a prescribed maximum strain value, the curve parameter, a_{req}, should be:

$$a_{\text{req}}=\frac{\varepsilon_{\max}^2}{\left(1-2\varepsilon_{\max}\right)^2\pi t^2} \tag{14}$$

The corresponding curve length becomes:

$$s_{\text{req}}=\sqrt{\frac{\pi}{a_{\text{req}}}}=\pi t\left(\frac{1-2\varepsilon_{\max}}{\varepsilon_{\max}}\right) \tag{15}$$

For $\varepsilon_{\max}$ = 2% and t = 2 [mm] the shape parameter a_{req} becomes equal to 34.5388 [mm^{-2}] and the curve length attains the value of 301.593 [m]. The outer side of the strip follows in essence the offset curve, as demonstrated in Eq. (8). The derived equations are based on the curvature of the outer (exposed) side of the strip, so the measured strain is the real one. With the given parameters, the maximum relative strain error occurs at the inner side that contacts the Euler-Fresnel curve (compressive strain). It remains however below 4% (Eq. (9)).

3 Experimental part

The Euler-Fresnel spiral has been made from aluminum according to a Catia® drawing which was based on the equations above. In this case the dimensions have been as mentioned above; they obviously may differ and result in a different spiral. For the initial test to validate this method, we have used a commercially known carbon/epoxy prepreg, here named A and an experimental carbon/epoxy prepreg, here named B, both kindly provided by Hexcel composites – UK. The coatings used for the initial tests are a polyurethane based standard coating, here named X and an experimental coating Y, which have been kindly provided by Akzo Nobel Aerospace coatings B.V., The Netherlands.

3.1 Sample dimensions, apparatuses and handling

Before performing the bending tests we have determined the E-modulus in the transversal direction and the strain at break (also in the transversal direction) of the carbon/epoxy composite laminates A and B at -55C° [12]. The given temperature is considered to be real usage temperature. E_A= 52000 [MPa]; ε_A at break = 1,27%; E_B= 60000 [MPa]; ε_B at break = 1,06%. The dimensions of the Euler-Fresnel test jig depend on the expected $\varepsilon_{\max}$ and thus on the resulting curvature. The thickness t and width b of the test samples are known; with $\varepsilon_{\max}$ = 2%, t = 2 [mm] and b = 20 [mm] the maximum contour length becomes 300 [mm]. The lay-up of the laminates can differ and is of essential influence on the material properties; we have worked with a laminate lay-up of $(0/90/0/90/0)_s$ with the outer layer transverse to the tensile direction. To determine the critical strain at room temperature and at low temperature such as -55 [°C], we bring the jig and the strip to the same temperature and slowly push the strip into the jig. The resulting micro-cracks can be detected by the penetrant method as described below. However, when we realized that the appearing cracks can acoustically be detected we

have monitored the strip during the bending process with an acoustical data acquisition system, LMS Roadrunner with PCB Piezotronics shear accelerometers model #333B30. At this point of our study we strongly believe that in the near future we will be able to determine the critical strain acoustically and even detect events that have not fully propagated to the surface, Fig.3.

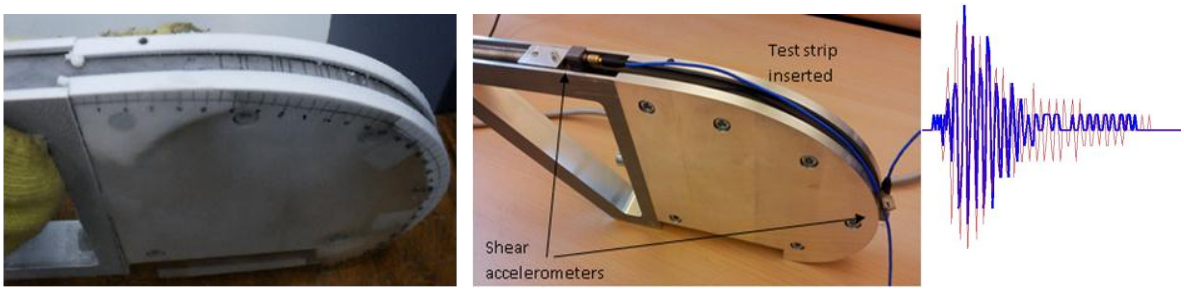

Figure 3. On the left: Euler-Fresnel jig with inserted test strip at -55C showing cracks; on the right Euler-Fresnel jig with inserted test strip and accelerometers with an acoustic crack-wave in volt vs. time

Appearing micro cracks are well visible on coated samples but not on uncoated. The micro cracks are detectable with the inverted microscope Axiovert 40 mat, using reflected-light brightfield. To determine the precise position of the very first crack (which we consider to be at the point of critical strain) dye penetrant inspection can be used.

3.1.1 Dye penetrant inspection

Dye penetrant inspection (DPI) is a widely applied and low-cost inspection method, Fig. 4, used to locate surface-breaking defects in all non-porous materials [11].

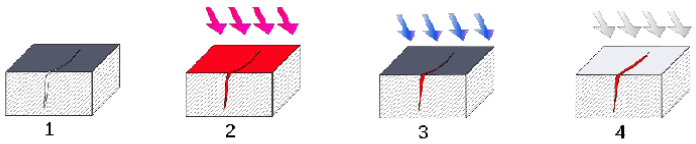

Figure 4. 1 SKC-S cleaner/Remover (petroleum distillates), 2 SKL-WP penetrant (petroleum distillates), 3 SKC-S cleaner/Remover (petroleum distillates), 4 Magnaflux spotcheck SDK-S2 developer

3.2 *Observations and results*

When stopping the bending process with the first cracking sound the strip is pulled out carefully, inspected under the microscope, and treated following the penetrant method. Very few cracks indicate the range of critical strain. When fully pushed into the jig the maximum strain of 2 % is achieved resulting in a saturation of crack density, Fig 5. The cracks clearly follow the pattern of the transverse fibers in the first ply.

Figure 5. Test strip 5 and 7 of Hexcel material A; the bold stripe shows the distance in the jig to the first crack: A-5 room temperature test stopped with first sound of crack; penetrant indicates two cracks; A-7 cold temperature test at -55° pushed fully into jig resulting in a high crack density

3.2.1 Cracks under the microscope

The micro cracks in the bended strips show dimensions of app. 5 [μm] width and 250 [μm] length; they are too small to be seen even by tomographic analysis. The micro cracks are initiated within the outer layer transverse to the tensile direction and propagate in direction of both sides, the second layer (parallel to the tensile direction) and the surface of the outer layer. We have found cracks that were not fully propagated yet, Fig 6b. When reaching the surface, the crack becomes visible.

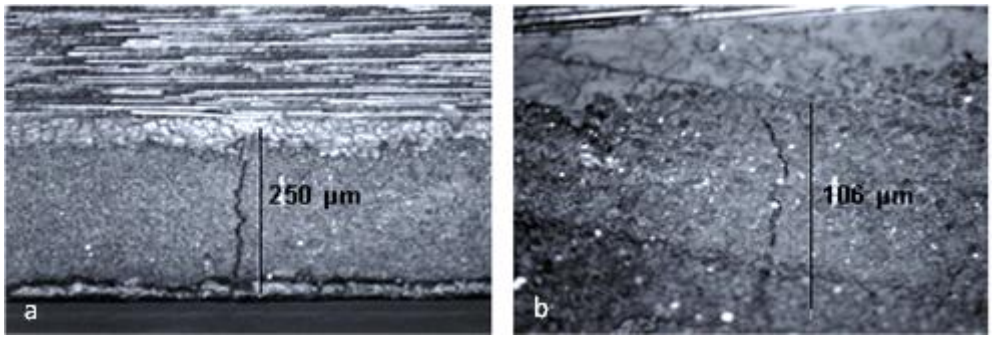

Figure 6. (a) micro crack in outer transversal layer, fully propagated to the surface (b) micro crack in outer transversal layer not fully propagated to the surface

Laminates with the outer layer directed parallel to the tensile direction show no cracks at low or at elevated temperatures, coated or uncoated.

3.2.2 Determination of strain$_{critical}$

All uncoated test strips have been treated with penetrant. According to Eq. (12), the distance to the very first crack is used as the parameter to calculate the resulting critical strain of the material. Table 1 shows the critical strain of carbon/epoxy laminates A and B uncoated and coated at room temperature and -55°C. The scatter in some cases is relatively high (up to 11%). For composite materials this has been noticed earlier and explained with the non-homogenous state [13]. Coated strips show nearly the same values for critical strain with also the same cracking pattern as the uncoated strips.

Critical strain [%]	**RT**	**-55°C**	**Coating X -55°C**	**Coating Y -55°C**	**Strain to break -55°C**
Carbon/epoxy A	0,51 +/- 0,06	0,39 +/- 0,01	0,48 +/- 0,05	0,5 +/- 0,02	1,27
Carbon/epoxy B	0,61 +/- 0,04	0,67 +/- 0,07	Not tested	0,75 +/- 0,05	1,06

Table 1. Results of Hexcel carbon/epoxy A and B when bended at RT and at -55°C. A has been coated with X and Y, wile B only has been coated with Y. Coated strips showed no cracks at RT when bended up to 2%.

3.2.3 Results and Discussion

It can be stated that in general material A shows lower critical strains than the experimental material B. The value of the critical strain decreases with 25% when bended at -55°C which can be explained by the β- and γ-transitions that occur at temperatures below T_g [14]. Modern epoxies match the specifications of the aeronautical industry in terms of ductility; however, when exposed to low temperatures a phase transition might take place which modifies the critical strain of the material.

Coating X has been tested on material A and B. At room temperature no cracks appeared up to 2% strain– however the sound of cracking could be detected. When tested at low

temperatures, the coating cracked at the same strain levels and the same cracking pattern as the uncoated strips. We consider this observation to be significant because it provides us with the evidence that cracking is initiated in the matrix of the composite which might even embrittle the coating layer. In former research [15] topcoat layers have always been considered as the more brittle ones which cause embrittlement of the layer underneath.

4 Conclusions

In this paper we have introduced the Euler-Fresnel spiral as an improved test method to measure critical strains and we have successfully demonstrated it's applicability. Besides we have made an approach to find a solution for the problem of cracks in the top layers on composite parts of airplanes by identifying the source of crack initiation. Using test strips with a slight angle of fiber direction will be the next step to prove the statement that cracks in the composite are acting as notches. Further work has to be done to determine critical strain levels of a variety of composite materials under different conditions. Various combinations of composite materials and top layers will have to be studied to eventually come to a solution to arrest the cracks and stop their propagation to the outer surface.

5 References

[1] Anemaat A, Spoormaker JL. Konstructieleer deel B. *Lecture notes (in Dutch), Delft University of Technology*, Delft (1989).
[2] Ishai O, Garg A, Nelson HG. *Nasa technical memorandum*, (August 1984).
[3] Ishai O, Garg A, Nelson HG. Hygrothermal Effects on the Mechanical Behaviour of Graphite Fibre-Reinforced Epoxy Laminates Beyond Initial Failure, *Composites*, **17**, | pp 23, (1986).
[4] Kambour RP. *J Polym Sci Macromol* (Rev 2008); **7**, issue1.
[5] Kramer EJ. *Environmental Cracking of Polymers*, Andrews EH (ed) "Developments in Polymer Fracture", Applied Science, London, pp 55–120 (1979).
[6] Altstädt V. The Influence of Molecular Variables on Fatigue Resistance in Stress Cracking Environments, *Advanced Polymer Science*, **188**, p.105–152 (2005).
[7] Vegt, AK van der. Kunststoffen. *Lecture notes (in Dutch), Delft University of Technology*, Delft, p. 47 (1982).
[8] Wyzgoski MG, Jacques CHM. Stress Cracking of Plastics by Gasoline and Gasoline Components, *Polymer engineering and science*, **17**, (1977), *No. 12.*
[9] Bergen jr, RL. Stress Cracking of Ridged Thermoplastics, *SPE journal*, **24**, pp. 77. (1968).
[10] Ziegler EE. *SPE Journal*, **10**, No. 4, p. 12 (april 1954).
[11] NEN-EN 571-1. *Non destructive testing- penetrant testing-part 1: general principles* (1997).
[12] ASTM D 790-10. *Standard test methods for flexural properties of unreinforced and reinforced plastics,* (2010).
[13] Bosma M. *Impact Properties of Coated Engineering Plastics*, PhD thesis, Faculty of Aerospace Engineering, Delft University of Technology, Delft, (1994).
[14] Pascault JP, Santereau H, Verdu J, Williams RJJ, *Thermosetting Polymers*, Marcel Dekker Inc., New York (2002), pp. 295-299.
[15] Rolland L, Broutman LJ, Surface Embrittlement of Ductile Polymers: A Fracture Mechanics Analysis, *Polymer Engineering and science*, **25**, (1985), pp. 207-211.